The MJO-Kelvin wave transition

A. H. Sobel[1,2,3] and D. Kim[3]

Received 30 July 2012; revised 18 September 2012; accepted 19 September 2012; published 23 October 2012.

[1] As the Madden-Julian oscillation (MJO) moves eastward from the Indian to the Pacific ocean, it typically accelerates, becomes less strongly coupled to convection, and becomes more similar to a dry Kelvin wave. This transition is analyzed using observations of outgoing longwave radiation and ERA Interim reanalyses of surface pressure and 850 hPa zonal wind. Two individual example events as well as composites are shown. The transitions are well defined, with distinct disturbances on either side of the transition whose identities as MJO or Kelvin waves are clear. In some cases there appears to be a pre-existing Kelvin wave passing through the MJO from the west to the east, but this feature is not apparent in the composites. The transitions occur at different longitudes in different events, over a wide range from the eastern Indian to the central Pacific oceans.
Citation: Sobel, A. H., and D. Kim (2012), The MJO-Kelvin wave transition, *Geophys. Res. Lett.*, *39*, L20808, doi:10.1029/2012GL053380.

1. Introduction

[2] Early theories for the Madden-Julian oscillation (MJO) portrayed it as an equatorial Kelvin wave whose properties were modified by the coupling of the large-scale circulation to deep convection [e.g., *Emanuel*, 1987; *Wang*, 1988]. More recently, many have come to be convinced that the MJO is fundamentally different from a Kelvin wave. One piece of evidence for this comes from the wavenumber-frequency analyses made popular by *Wheeler and Kiladis* [1999], which show that the MJO and "convectively coupled Kelvin waves" occupy distinctly different parts of the spectrum.

[3] Fourier spectra obscure geographic variability in both the MJO itself and the mean climate within which it exists, however. Measured by its amplitude in fields directly related to convection — precipitation, outgoing longwave radiation (OLR), and the like — the MJO has its largest amplitude over the Indian and western Pacific oceans.

[4] Over the western hemisphere — apart from the eastern Pacific in northern summer [*Knutson et al.*, 1986; *Maloney and Kiehl*, 2002] — the MJO modulates convection much more weakly and propagates faster than it does over the Indian and western Pacific [*Hendon and Salby*, 1994; *Milliff and Madden*, 1996; *Bantzer and Wallace*, 1996; *Kiladis et al.*, 2005]. These fast eastward signals have the characteristics of a Kelvin wave radiating into the western hemisphere from MJO convection in the eastern hemisphere [*Hendon and Salby*, 1994; *Matthews*, 2000]. Viewed from the framework of dry dynamics, the dynamical response to the MJO convection is "forced" in the eastern hemisphere while the radiated Kelvin wave in the western hemisphere is "free" [*Hendon and Salby*, 1994, 1996]. This is evident in their different relationships between wind and pressure. Westerlies are coincident with high pressure in a Kelvin wave. The opposite is more nearly true for the MJO, and is indicative of strong dissipation in the zonal momentum budget [*Lin et al.*, 2005]. With its typically large phase speed (30–40 ms^{-1}) and weak OLR signal, the free Kelvin wave also appears in several studies [*Milliff and Madden*, 1996; *Bantzer and Wallace*, 1996; *Kiladis et al.*, 2005] to be coupled to convection more weakly than are the "convectively coupled Kelvin waves" studied by many authors [e.g., *Kiladis et al.*, 2009].

[5] We are led to the view that the MJO truly exists as a phenomenon distinct from Kelvin waves only in a limited region. When an MJO disturbance reaches the easternmost limit of that range, we might say it ceases to exist as the MJO but emits a Kelvin wave. From the literature one has the impression that the transition occurs over the Pacific [*Milliff and Madden*, 1996; *Matthews*, 2000; *Kiladis et al.*, 2005].

[6] *Roundy* [2012] analyzes the composite dynamical structures of disturbances over the Indian ocean (60–90E) with the spectral properties of convectively coupled Kelvin waves as a function of apparent phase speed. He focuses on the relationship between surface pressure and low-level zonal wind. As the phase speed varies, Roundy finds that the phase relationship between wind and pressure changes in a way which is more consistent with a continuous change in the dynamical character of individual disturbances as a function of phase speed, as opposed to distinct Kelvin and MJO disturbances whose representations in the population vary with phase speed. This suggests that "pure" Kelvin and MJO disturbances exist only as end members of a continuous spectrum of disturbances which share some characteristics of both, becoming more Kelvin-like as phase speed increases.

[7] On the other hand, we might consider the hypothesis that the continuous transition in pressure-wind relationships found by Roundy could be partly attributable to pure MJO disturbances transitioning to pure Kelvin waves with a short-lived hybrid phase in between, rather than only to long-lived, dynamically distinct hybrid disturbances. We find here that the transitions occur frequently over the Indian ocean, so that limiting the analysis to this region does not exclude them from the analysis.

[8] In this study we analyze the transitions of MJO disturbances into fast ($\sim$30 ms^{-1}) Kelvin wave disturbances. Alternatively we might describe this process as emission of

[1]Department of Applied Physics and Applied Mathematics, Columbia University, New York, New York, USA.
[2]Department of Earth and Environmental Sciences, Columbia University, New York, New York, USA.
[3]Lamont-Doherty Earth Observatory, Earth Institute at Columbia University, Palisades, New York, USA.

Corresponding author: A. H. Sobel, Department of Applied Physics and Applied Mathematics, Columbia University, New York, NY 10027, USA. (ahs129@columbia.edu)

0094-8276/12/2012GL053380

fast Kelvin waves from terminating or weakening MJO disturbances. We focus on the OLR, surface pressure and low-level wind fields. The phase relationship between the latter is particularly useful for distinguishing MJO disturbances from Kelvin waves. Our interest is in visualizing the spatiotemporal structure of Kelvin wave emission, determining the degree to which it is localized in both space and time, and quantifying the frequency of its occurrence as a function of longitude and season.

2. Data and Methods

2.1. Data

[9] We use daily-averaged outgoing longwave radiation (OLR) from the Advanced Very High Resolution Radiometer [*Liebmann and Smith*, 1996] as a proxy of deep convection in the tropics. We use daily 850-hPa zonal wind and surface pressure (p_s) from the European Centre for Medium-Range Weather Forecasts (ECMWF) Reanalysis-Interim (ERA-Interim) [*Dee et al.* 2011]. Data during the period of 1979–2009 are used. The climatological seasonal cycle was removed from all fields to obtain daily anomalies. The resulting anomalies were then filtered by Fourier and inverse-Fourier transforms [*Wheeler and Kiladis*, 1999] to retain only components that have 20–100 day periods and eastward propagating zonal wavenumbers 1–9, a range which encloses the MJO spectral signal.

2.2. Methods

[10] The filtered OLR and p_s anomalies were used to identify transition events. Two polarities of such events, depending on the sign of p_s anomalies, were identified separately. Here we describe the method applied in the case of negative p_s anomalies. The method for positive p_s anomalies is identical, with signs of all fields reversed. After averaging the p_s anomalies between 15°S and 15°N, we find the minimum value and the longitude where the minimum is located on each day. Using this information along with knowledge from past studies, we searched for the days that satisfy the following conditions:

[11] 1. The minimum value of the filtered OLR anomaly is less than -20 Wm^{-2} from Day -2 to Day 0.

[12] 2. The distance between the longitudes of minimum OLR and p_s is less than 12.5 degrees during the period from Day -1 to Day 0. In other words, the p_s minimum is near the OLR minimum before the emission of the Kelvin wave. This criterion, combined with the preceding one, ensures the existence of a relatively strong MJO event.

[13] 3. The longitudinal distance between the p_s minima on Day 0 and Day +1 is greater than that between the OLR minima during the same period plus 10 degrees. In other words, the separation of the low pressure from the convection must occur rapidly.

[14] 4. The minimum p_s is located more than 40 degrees east of the minimum OLR on Day +5. Given the typical phase speeds of the disturbances involved, this means we search for events in which the minimum p_s propagates eastward with a phase speed greater than that of the OLR minimum for at least 3–5 days.

[15] With these criteria, there are 56 transition events for OLR minima out of 140 MJO events (those which satisfy the first criterion above, without necessarily satisfying any of the others) altogether in the record, or 40%. For OLR maxima, there are 51 events out of 115, or 44%. The transition, defined as above, is not a rare occurrence.

3. Results

[16] Figures 1 and 2 show two individual events. We denote each event by the date at which the Kelvin wave separates from the MJO according to the criteria given above. In Figure 1, June 3 1982 is shown as Day 0, while in Figure 2 November 28 2009 is shown. Figures 1a and 2a show Hovmoeller plots of surface pressure, zonal wind at 850 hPa, and OLR. Figures 1b and 2b show the longitudes of local minima in OLR, p_s, and zonal wind.

[17] In Figures 1a and 2a we can identify the active MJO phases by the global OLR minima at each time. They move eastward with slow speeds typical of the MJO, a few meters per second. Prior to day zero, the winds are westerly and pressures are low within these OLR minima. In Figure 1a, the pressure in the OLR minimum switches from low to high between days +5–10, while in Figure 2a it remains low as the slow disturbance continues further east. In both cases the wind remains westerly within the region of lowest OLR. In both cases, between around day -10 and day 0 a pressure minimum separates from the OLR minimum and moves eastward much more rapidly. These fast-moving pressure minima are associated primarily with easterlies. We interpret these faster-moving disturbances as Kelvin waves emitted by the MJO.

[18] In both Figures 1a and 2a, the OLR minima have adjacent OLR maxima indicating anomalously suppressed convection. Before day 0, the OLR maxima are to the east of the minima, while after that those OLR maxima decrease in amplitude and new maxima appear to the west of the OLR minima. Both figures also show indications of fast-moving pressure perturbations to the west of the OLR minima prior to day 0. These suggest that the Kelvin waves separating from the MJO after day 0 may not have originated with the MJO, but rather passed through it. We see below, however, that this feature is not present in the composite anomalies constructed from many events.

[19] Figures 1b and 2b indicate the longitudes of local minima in pressure, OLR, and zonal wind, to illustrate the behavior described above in more schematic form. We see that before day zero the OLR and pressure minima are nearly coincident. The wind minima are roughly 30 degrees to the east. Later, the wind and pressure minima remain closely associated with each other but separate from the OLR minima. The propagation appears to be by a combination of periods of slow motion and fast eastward jumps. We do not interpret this detail too literally, as the position of a minimum can be a noisy quantity. Overall, the propagation is eastward at an average speed on the order of 30 ms^{-1}, broadly similar to that found in previous studies [*Milliff and Madden*, 1996; *Matthews*, 2000; *Kiladis et al.*, 2005].

[20] Figure 3a shows a composite of all 56 events defined by OLR minima (and the other associated criteria). The longitudes of the OLR minima are used to align the composite fields. The primary features of the two individual events shown in Figures 1 and 2 are still present, but with less additional finer structure to complicate the picture. (Composites constructed from unfiltered data on the same sets of dates are qualitatively similar and are shown in

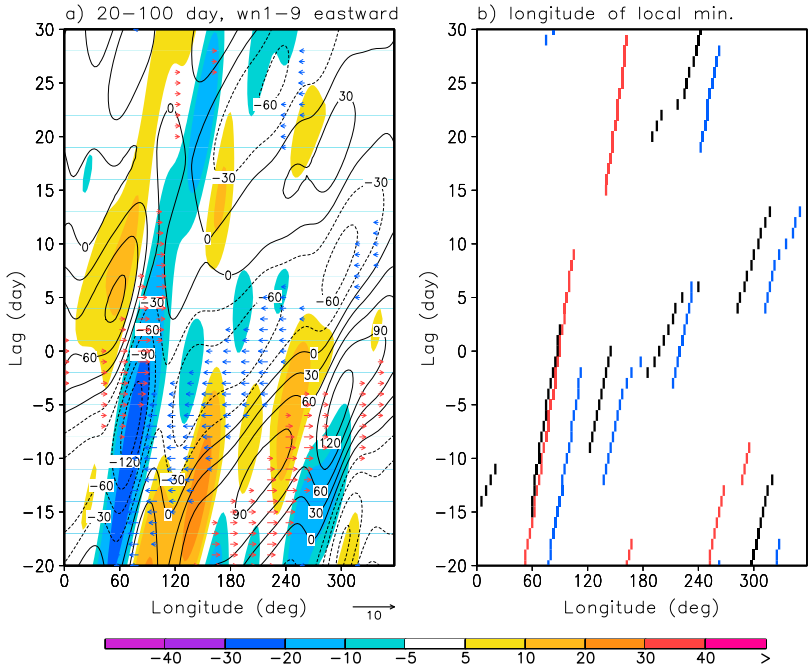

Figure 1. Longitude-time Hovmoeller plot for an MJO event centered (day 0) on June 3 1982. (a) Surface pressure p_s (Pa), zonal wind at 850 hPa m∼s^{-1} and OLR W∼m^{-2} are shown. All fields are band-pass filtered to 20–100 day frequencies in time and eastward-propagating zonal wave numbers 1–9 in space, and averaged over 15°S–15°N. (b) Lines track the local minima in OLR (red) surface pressure (black) and maxima in zonal wind (blue) in the fields shown in Figure 1a.

Figure S1 in Text S1 of the auxiliary material.)[1] We see the slow-moving OLR minimum with associated westerlies and low pressure before day 0, and the faster-moving low pressure with associated easterlies and very little OLR signal separating around day 0. Perhaps more clearly than in the individual events, we see the composite westerly anomaly persist in its slow eastward motion after day 0; at this time the OLR anomaly weakens and the pressure associated with the westerlies becomes small or positive. Also as in the individual events, the OLR maximum east of the minimum decays around day zero while a new maximum develops to the west around that time.

[21] Figure 3b shows a composite as in Figure 3a, but based on the 51 OLR maxima (suppressed phases of the MJO) rather than minima. To a large extent the picture is similar to that in Figure 3a with all signs simply reversed, but there are some differences. The easterly winds near the OLR maximum in Figure 3b are weaker than the westerly winds near the OLR minimum in Figure 3a, and the OLR minimum east of the maximum before day 0 in Figure 3b is stronger than the maximum east of the minimum before day 0 in Figure 3a. Both of these differences are consistent with a moderate degree of nonlinearity in the MJO (when it is not defined by linear diagnostics which insure equality of positive and negative anomalies by construction), with the active phase being the stronger. Figure S2 shows that these differences, measured by the difference between the results in Figure 3a and minus the results in Figure 3b, are statistically significant.

[22] In both Figures 3a and 3b one is hard-pressed to find indications of pre-existing fast-moving Kelvin wave signals impinging on the MJO disturbance from the west prior to day 0. Any such disturbances either do not occur systematically enough, or do not occur with consistent enough phase relationships relative to the outgoing Kelvin wave to appear in the composites. This implies that such incoming Kelvin waves are not essential to the transition process, and that we can view the outgoing Kelvin wave as being generated by the MJO.

[23] Figure 4a shows the distribution of longitudes at which the separation of Kelvin and MJO anomalies occurs, by the definitions given above. Distributions for OLR minima and maxima are given separately. The most separations in any 30-degree longitude band occur in the range 60–90E, over the eastern Indian ocean. This longitude range was the focus of *Roundy* [2012]. There is a broader maximum over the Maritime continent and western Pacific, however, which altogether accounts for more total separations than occur over the Indian ocean. There are almost none over the eastern Pacific, Atlantic, Americas, or Africa. This is consistent with our prior conception of the MJO's existence as a mode distinct from Kelvin waves only over the Indian, Maritime continent, and western Pacific regions.

[24] Figure 4b shows the distribution of separations by calendar month. There is a minimum in northern summer which is consistent with the known minimum in MJO activity (as defined by equatorially-centered diagnostics) in that period.

4. Conclusions

[25] We have performed an analysis of the transitions of tropical intraseasonal disturbances from MJO to fast Kelvin waves. The MJO disturbances are characterized by slower propagation, stronger OLR anomalies, and spatial coincidence

[1]Auxiliary materials are available in the HTML. doi:10.1029/2012GL053380.

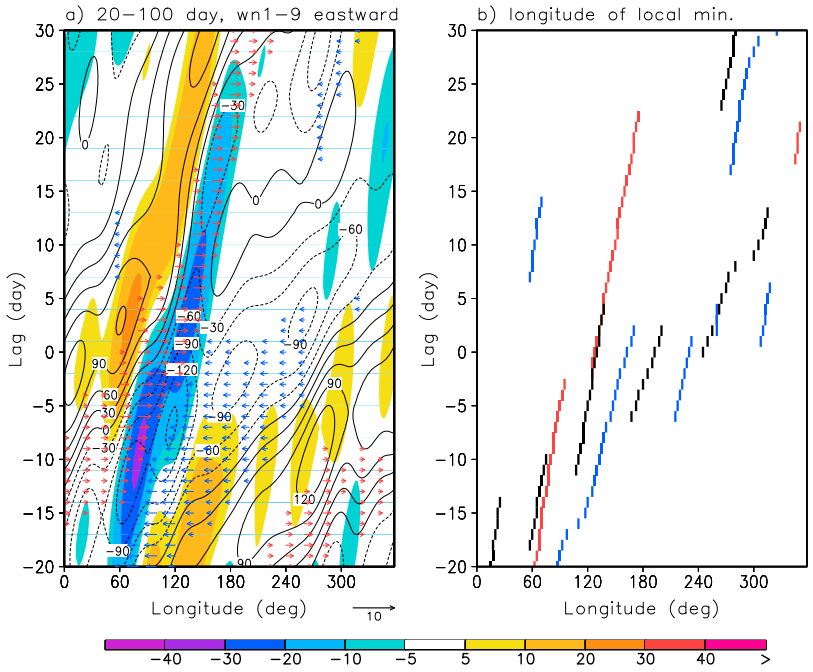

Figure 2. As in Figure 1, but for an event centered on November 28, 2009.

of surface low pressure with low-level westerly winds; the Kelvin waves by faster propagation, much weaker OLR anomalies, and coincidence of surface high pressure with low-level westerlies. We have presented two individual cases as well as composites based on a set of subjectively defined but objectively applied criteria.

[26] The transitions are fairly sharply defined, with distinct disturbances on either side of the transition whose identities as MJO or Kelvin waves are clear. The transitions occur at different longitudes in different events, over a wide range from the eastern Indian to the central Pacific oceans.

[27] Our analysis was designed to find transitions between MJO and fast Kelvin waves, and not to identify disturbances whose characteristics are mixtures of both. Our analysis thus does not refute the conclusion of [*Roundy*, 2012] that a continuous spectrum of such hybrid disturbances exists. It does

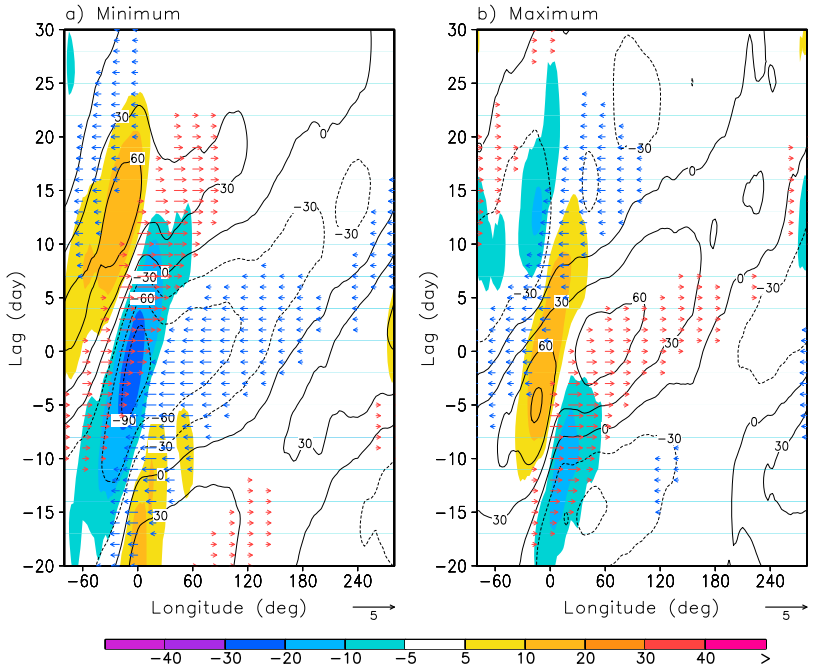

Figure 3. As in Figures 1a and 2a, but for composite events, constructed according to criteria described in the text: (a) for composite events centered on anomalously low OLR (active MJO phases), and (b) centered on anomalously high OLR (suppressed MJO phases). Longitude on the *x*-axis is not absolute as in Figures 1 and 2, but relative to the longitude of the p_s minimum (Figure 3a) or maximum (Figure 3b) on day 0.

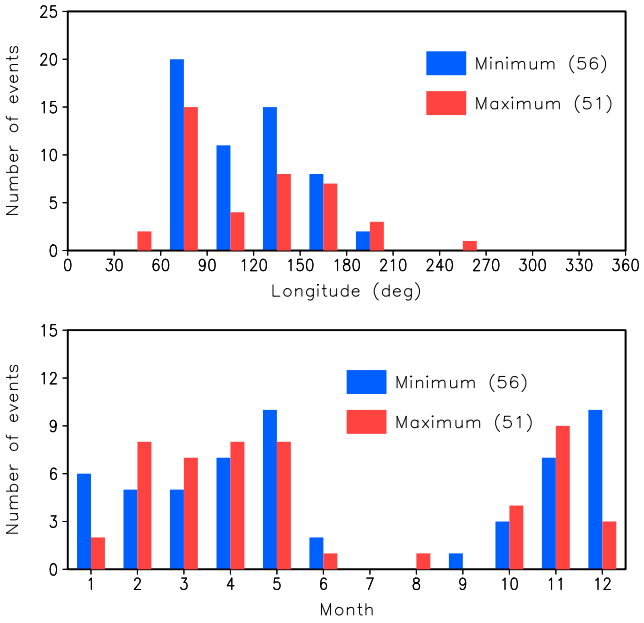

Figure 4. Histograms showing (a) the longitudes and (b) calendar months at which the MJO-Kelvin wave transitions occur, according to criteria given in the text. Blue and red bars show results for OLR minima and maxima respectively.

lead us to speculate, however, that some hybrid disturbances could be transitory disturbances undergoing a transition from essentially a pure MJO to a pure Kelvin wave, and taking on intermediate properties only during the transition.

[28] **Acknowledgments.** We thank Paul Roundy for discussions that helped to motivate this work, and George Kiladis and Juliana Dias for comments and suggestions on the manuscript. This work was supported by NASA grant NNX09AK34G, NOAA grant NA08OAR4320912 A6R, NSF grant AGS-1062206, and ONR grant N00014-12-1-0911.

[29] The Editor thanks George N. Kiladis and an anonymous reviewer for their assistance in evaluating this paper.

References

Bantzer, C. H., and J. M. Wallace (1996), Intraseasonal variability in tropical mean temperature and precipitation and their relation to the tropical 40–50 day oscillation, *J. Atmos. Sci.*, *53*, 3032–3045.

Dee, D. P., et al. (2011), The ERA-Interim reanalysis: Configuration and performance of the data assimilation system, *Q. J. R. Meteorol. Soc.*, *137*, 553–597.

Emanuel, K. A. (1987), An air-sea interaction model of intraseasonal oscillations in the tropics, *J. Atmos. Sci.*, *44*, 2324–2340.

Hendon, H. H., and M. L. Salby (1994), The life cycle of the Madden-Julian oscillation, *J. Atmos. Sci.*, *51*, 2225–2237.

Hendon, H. H., and M. L. Salby (1996), Planetary-scale circulations forced by intraseasonal variations of observed convection, *J. Atmos. Sci.*, *53*, 1751–1758.

Kiladis, G. N., K. H. Straub, and P. T. Haertel (2005), Zonal and vertical structure of the Madden-Julian oscillation, *J. Atmos. Sci.*, *62*, 2790–2809.

Kiladis, G. N., M. C. Wheeler, P. T. Haertel, K. H. Straub, and P. E. Roundy (2009), Convectively coupled equatorial waves, *Rev. Geophys.*, *47*, RG2003, doi:10.1029/2008RG000266.

Knutson, T. R., K. M. Weickmann, and J. E. Kutzbach (1986), Global-scale intraseasonal oscillations of outgoing longwave radiation and 250-mb zonal wind during Northern Hemisphere summer, *Mon. Weather Rev.*, *114*(3), 605–623.

Liebmann, B., and C. A. Smith (1996), Description of a complete (interpolated) outgoing longwave radiation dataset, *Bull. Am. Meteorol. Soc.*, *77*, 1275–1277.

Lin, J.-L., M. Zhang, and B. E. Mapes (2005), Zonal momentum budget of the Madden-Julian oscillation: The source and strength of equivalent linear damping, *J. Atmos. Sci.*, *62*, 2172–2188.

Maloney, E. D., and J. T. Kiehl (2002), MJO-related SST variations over the tropical eastern Pacific during Northern Hemisphere summer, *J. Clim.*, *15*(6), 675–689.

Matthews, A. J. (2000), Propagation mechanisms for the Madden-Julian oscillation, *Q. J. R. Meteorol. Soc.*, *126*, 2637–2652.

Milliff, R. F., and R. A. Madden (1996), The existence and vertical structure of fast, eastward-moving disturbances in the equatorial troposphere, *J. Atmos. Sci.*, *53*(4), 586–597.

Roundy, P. E. (2012), Observed structure of convectively coupled waves as a function of equivalent depth: Kelvin waves and the Madden-Julian oscillation, *J. Atmos. Sci.*, *69*, 2097–2106.

Wang, B. (1988), Dynamics of tropical low-frequency waves: An analysis of the moist Kelvin wave, *J. Atmos. Sci.*, *45*, 2051–2065.

Wheeler, M., and G. N. Kiladis (1999), Convectively coupled equatorial waves: Analysis of clouds and temperature in the wavenumber-frequency domain, *J. Atmos. Sci.*, *56*, 374–399.